Performance Analysis of Spectral-Phase-Encoded Optical CDMA System Using Two-Photon-Absorption Receiver Structure for Asynchronous and Slot-Level Synchronous Transmitters

Kambiz Jamshidi, *Member, IEEE*, and Jawad A. Salehi, *Senior Member, IEEE*

***Abstract*—In this paper, we analyze the performance of a nonlinear two-photon-absorption (TPA) receiver and compare its performance with that of a single-photon-absorption (SPA) receiver in the context of spectral-phase-encoded optical code-division multiple access (CDMA) technique. The performances for the above systems are evaluated for two different transmission scenarios, namely, asynchronous and slot-level synchronous transmitters. Performance evaluation includes different sources of degradation such as multiple-access interference, noise due to optical amplification, shot noise, and thermal noise. In obtaining the performance, the mean and variance of the received signal in each of the above techniques are derived, and bit error rate is obtained using Gaussian approximation. In general, it is shown that TPA receivers are superior in performance with respect to SPA receivers when the receiver employs a much slower photodetector in comparison with the laser's transmitted pulse duration. This, indeed, is the reason behind the choice of nonlinear receivers, such as TPA, in most spectral-phase-encoded optical CDMA systems.**

***Index Terms*—Asynchronous transmission, bit-error-rate (BER) analysis, nonlinear receiver, optical code-division multiple access (CDMA), spectral-phase-encoded optical CDMA, synchronous transmission, two-photon absorption receiver.**

I. Introduction

THE HERCULEAN task of satisfying bandwidth hungry services by many millions of customers all over the world will undoubtedly push optical-fiber medium toward customers' home or business addresses [1], [2]. Furthermore, ubiquitous use of fiber-optic medium in long-haul and metropolitan-based telecommunications networks worldwide is making fiber-to-the-home or curb technology a natural choice for the next wave in telecom investment and customer demand satisfaction [2]. To satisfy the above trend in delivering extraordinary high bandwidth services to each individual customer would ultimately require networks that operate without any electronic processing at their intermediate stages, and all key processing functions such as mux/demux, add-drop module, switching, filtering, encoding/decoding, etc., are established in the all-optical domain [3]. Among the few alternatives available for the access technology at the local loop level, all-optical passive star networks are capturing the most attention due to their use of mostly passive optical components and the ease with which they are implemented and maintained [3].

The blitzing success of code-division multiple access (CDMA) technique in wireless and cellular communications network may once again prove its superiority over other access techniques in all-optical fiber-based access networks [4]. Optical CDMA enjoys from many features that are of immense interest, for example, simplified and decentralized network control, enhanced information security, improved spectral efficiency, and increased robustness in multirate services [4]–[14]. Among many optical CDMA techniques introduced to date, none are as powerful as the spectral-phase-encoded ultrashort light pulse CDMA or femtosecond CDMA technique when access networks require to deliver ultrahigh rate services to their corresponding customers [5], [9], [11], [13]–[16]. However, enabling technologies that need to support such advanced systems are ongoing research topics. On the other hand, as advanced devices become more mature for use in such systems, one needs to extract their fundamental mathematical models in the context of statistical communication theory to predict their performance in a network prior to their implementation as function of key system parameters such as bit error rate (BER), signal-to-noise ratio, multiple-access interference (MAI), code length, threshold, etc., [11], [19].

In this paper, building upon the previously introduced statistical model for nonlinear two-photon-absorption (TPA) devices [19], we obtain the performance of employing TPA devices for detecting ultrashort light pulses in the context of spectral-phase-encoded optical CDMA system. TPA devices are used in receivers to distinguish between correctly decoded and incorrectly decoded pulses in the spectral-phase-encoded optical CDMA system. The performance comparison of systems using TPA receivers versus single-photon-absorption (SPA) receivers is the subject and the scope of this paper. Recently, a slot-level synchronous transmission was introduced for spectral-phase-encoded optical CDMA system to decrease the number of interfering users by reducing the total interference signal

Manuscript received July 11, 2006; revised October 28, 2006. This work was supported in part by the Hi-Tech Industries Center of Iran and ITRC.

The authors are with the Optical Networks Research Laboratory, Electrical Engineering Department, Sharif University of Technology, Tehran 11365-8639, Iran (e-mail: jamshidi@mehr.sharif.edu; jasalehi@sharif.edu).

Digital Object Identifier 10.1109/JLT.2007.896789

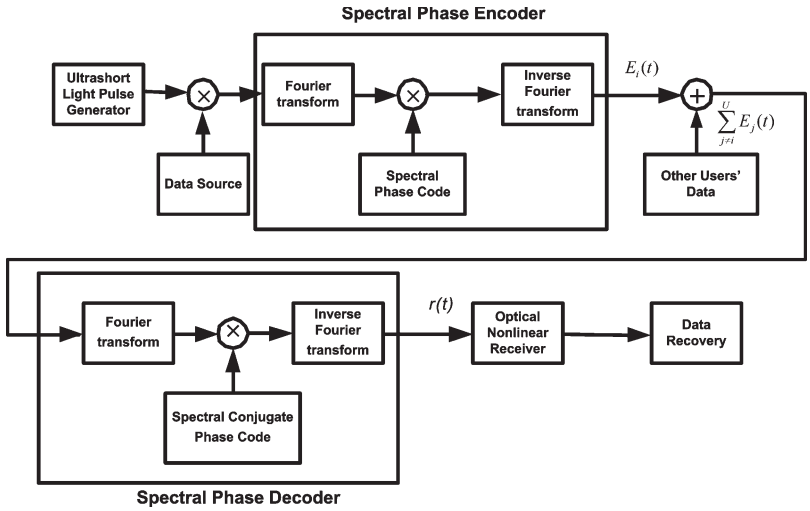

Fig. 1. Typical block diagram of spectral-phase-encoded CDMA.

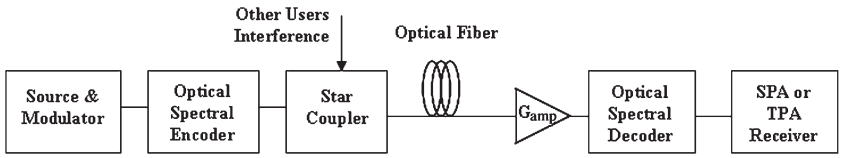

Fig. 2. Schematic of spectral-phase-encoded CDMA using optical amplifier.

among different users in the system, which leads to an improved performance of the system [8]. The performance of TPA and SPA receivers are obtained and compared, in this paper, by using slot-level synchronous and asynchronous transmitters with typical and ideal photodetection speed.

In Section II of this paper, we briefly describe the spectral-phase-encoded optical CDMA system to be used in our performance analysis. Section III describes the SPA and TPA receiver structures used at the receiving end of the above systems. Furthermore, we obtain the means and variances of interfering signal at the output of each SPA and TPA receivers. Section IV evaluates the performance of the aforementioned system for two distinctly different transmission scenarios, namely, slot-level synchronous and asynchronous transmissions. We discuss the results in Section IV-C and conclude this paper in Section V.

II. Spectral-Phase-Encoded Optical CDMA

A typical spectral-phase-encoded optical CDMA system is shown in Fig. 1. The Fourier transform of a band-limited transmitted pulse can be interpreted as a sum of N_0 frequency bins. Each frequency bin has a bandwidth equal to $\Delta\omega$, which leads to the total bandwidth of $W = N_0\Delta\omega$ [5]. In the spectral-phase-encoded technique, an encoder multiplies each frequency bin by 1 or -1. This implies that, for example, the phase of the mth frequency bin of the ith user receives a phase shift equal to φ_i^m, which can be either 0 or π. By employing a star coupler, the information of each user is broadcasted to all users. The decoder of the ith receiver is similar to its encoder, with a phase code that is equivalent to its corresponding complex conjugate. Fig. 2 shows a spectral-phase-encoded optical CDMA system using an optical amplifier. As discussed in [11], the desired locations in placing an optical amplifier in a spectral-phase-encoded system are those which are either before or after the optical star coupler. By using a single optical amplifier in the network and by minimizing fiber nonlinearity, the optical amplifier is placed after the star coupler in the system.

Therefore, the received signal at the input of the ith receiver $r(t)$ can be expressed as [11]

$$r(t) = \sqrt{G}E_{ii}(t) + \sqrt{G}\sum_{j\neq i}^{U} E_{ij}(t) + Q(t) \qquad (1)$$

where G, the gain, is the total amplification and losses along the path. As described in [11], $G = G_{\rm amp}L_1L_2/U$, where $G_{\rm amp}$ is the gain of the amplifier in use, L_1 is the total loss before the amplification, L_2 is the total loss after the amplification, and U is the total number of users, and for simplicity, it also indicates the size of the star coupler used in the network. $Q(t)$ is the amplification noise present at the receiver end with power spectral density N_T. $E_{ii}(t)$ is the properly decoded signal, and $\sum_{i\neq j}^{U} E_{ij}(t)$, the MAI, is the improperly decoded signal due to all other users in the network. By using the method presented in [11], the power spectral density N_T of $Q(t)$ is equal to $n_{\rm sp}(G_{\rm amp}-1)L_2$ for the system shown in Fig. 2.

III. SPA and TPA Receiver Structures

Recently, several optical devices in gating the received optical short pulses with applications in optical time-division multiple access were introduced [13]. By using such gating optical devices, it is possible to detect pulses with duration as low as several picoseconds. In our system modeling, we

consider the use of an ideal gating device for SPA receiver structure whenever needed. This assumption is made in order to simplify the mathematical model of the receiver structure, in comparing the performance of SPA and TPA receivers. For our system performance comparison, the mean and the variance of the properly and improperly decoded received signals using the SPA and TPA receivers are obtained.

A. SPA Receiver

The received number of photoelectrons in the spectral-phase-encoded optical CDMA system $Y_{i,\mathrm{SPA}}$, by choosing a method similar to [11] and [17], can be described as (see Appendix A)

$$Y_{i,\mathrm{SPA}} = \frac{\eta T}{2} \sum_{n=1}^{M} \left((a_n + x_{\mathrm{cn}})^2 + x_{\mathrm{sn}}^2 \right) \tag{2}$$

where η is the quantum efficiency of the photodetector, and M is the number of modes in the received signal $r(t)$, which depends on the speed of the receiver photodetector [17]. a_n is the nth component of the base-band representation of the received signal, and x_{cn} and x_{sn} are the real and the imaginary components of the base-band representation of the accumulated noise due to amplification in erbium-doped fiber amplifier and the MAI signal, as described in Appendix A. The variance for each component noise term is equal to N_S/T, whereas their corresponding mean is equal to zero. Assuming that the mean number of the transmitted photons of the ith user is equal to m, the received amplified signal can be expressed as $(T/2)\sum_{n=1}^{M} a_n^2 = mG$ [17]. In the absence of any optical amplification gain and losses in the system, each interfering user's signal at the output of the desired user's decoder is modeled as a Gaussian random variable with a power spectral density equal to m/N_0 [5], [11]. Therefore, the noises due to optical amplification and l amplified interfering users can be added to form a noiselike Gaussian variable with a power spectral density equal to N_S, which can be expressed as [11]

$$N_S = N_T + l\frac{mG}{N_0}. \tag{3}$$

The mean and the variance of the received signal assuming shot noise can be expressed as [17]

$$E\{Y_{i,\mathrm{SPA}}\} = \eta mG + \eta M N_S \tag{4}$$

$$\mathrm{Var}\{Y_{i,\mathrm{SPA}}\} = \eta mG + \eta M N_S + 2\eta^2 mGN_S + \eta^2 M N_S^2. \tag{5}$$

B. TPA Receiver

In a TPA receiver, an electron will be liberated from a photodetector when two photons are incident on the TPA photodetector simultaneously [9], [10]. A medium with a band gap less than twice the frequency of the incoming signal is used for such TPA photodetectors [18]. It is shown that the number of photoelectrons N, which is generated by a TPA photodetector in a period Δt, is proportional to the square of the incident intensity of the light pulse, i.e., $I^2(t) = |r(t)|^4$, in addition to the intensity $I(t) = |r(t)|^2$, i.e., [18]

$$N = \int_0^{\Delta t} \left(\frac{\alpha}{hf} I(t)dt + \frac{\gamma}{2hf} I^2(t) \right) dt \tag{6}$$

where α and γ are constants relating to SPA and TPA coefficients, h is the Planck's constant, and f is the frequency of the incident light. An in-depth mathematical analysis and modeling of such receivers was presented in [19]. From Appendix B and by using the methodology presented in [19], the mean and the variance of the received ith user's signal for an ideal TPA photodetector, i.e., $\alpha = 0$, can be expressed as

$$E(Y_{i,\mathrm{TPA}}) = k_3 \left(m^2G^2 + 4mGN_S + 2MN_S^2 \right) \tag{7}$$

$$E\left(Y_{i,\mathrm{TPA}}^2\right) = k_3^2 \left(m^4G^4 + 16m^3G^3N_S + 72m^2G^2N_S^2 + 96mGN_S^3 + 24MN_S^4 \right) \tag{8}$$

where k_3 is defined in [19] as $k_3 = 12Vhf\gamma/16S^2T$. In this equation, V is the volume of the detector, T is the integration time of the photodetector, and S is the area of the TPA photodetector. Including the shot noise, the variance of the received signal is equal to the mean of the squared signal minus the square of the mean received signal plus the mean of the received signal, i.e.,

$$\mathrm{Var}(Y_{i,\mathrm{TPA}}) = \underbrace{E(Y_{i,\mathrm{TPA}})}_{\text{due to shot–noise}} + \left\{ E\left(Y_{i,\mathrm{TPA}}^2\right) - E^2(Y_{i,\mathrm{TPA}}) \right\}. \tag{9}$$

IV. Performance Evaluation

The performance of both SPA and TPA receiver structures, given l interfering users for the desired user, can be expressed as [17]

$$\mathrm{BER}(l) = \frac{1}{2}Q\left(\frac{E(Y_{1,l}) - \mathrm{Th}}{\mathrm{Var}(Y_{1,l})} \right) + \frac{1}{2}Q\left(\frac{\mathrm{Th} - E(Y_{0,l})}{\mathrm{Var}(Y_{0,l})} \right) \tag{10}$$

where $Y_{1,l}$ is the received signal when the transmitted bit is equal to 1 and there are l interfering users, and $Y_{0,l}$ is the received signal when the transmitted bit is equal to 0 and there are l interfering users. Th is the threshold value for the decision variable, and it is optimized to minimize the overall BER. Including thermal noise, the variance for this noise, which is equal to $(4 \cdot k_{\mathrm{B}} \cdot T_r \cdot T)/e^2R_L$, is added to the variance of the received signal. In this expression, T is the integration time period, k_{B} is Boltzman constant, T_r is the equivalent temperature of the receiver, e is the electron charge, and R_L is the resistance of the load which is seen from the photodetector input [17]. Given the BER(l) in (10), we obtain the BER of the system for two different cases of asynchronous and slot-level synchronous transmitters for both the SPA and TPA receiver structures.

A. Asynchronous Transmitter

In this case, different transmitters in the system are not coordinated in their corresponding time of information transmission. This leads to a uniform distribution of the initial transmission time within a bit period. The probability that an improperly decoded pulse will interfere with the properly decoded pulse for a system utilizing asynchronous transmitters is equal to $1/2K$, where, from [5], K is a parameter describing the ratio between the bit time to that of the spread signal, i.e., $K = T/N_0T_c$. Therefore, the probability that l users interfere with the desired user can be written as [5]

$$P_{\text{Async}}(l) = \binom{U-1}{l}\left(\frac{1}{2K}\right)^{l}\left(1-\frac{1}{2K}\right)^{U-1-l} \tag{11}$$

and the BER of the system can be expressed as

$$\text{BER} = \sum_{l=0}^{U-1} P_{\text{Async}}(l)\text{BER}(l). \tag{12}$$

B. Slot-Level Synchronous Transmitter

As described in [8], the asynchronous transmission suffers from the interfering among the desired user's signal and other users' signal in the network. A slot-level transmission is suggested to decrease this interfering effect. In this scheme, different transmitters are coordinated with each other in the slot-level transmission, i.e., in the duration of an encoded pulse, N_0T_c. Although the transmitters' complexity is higher in this case, the effective number of interfering users decreases, hence enhancing the system performance when compared with the asynchronous transmission case.

In slot-level transmission scheme, the total number of interfering users is, at most, equal to $\lceil U/K \rceil - 1$, where $\lceil x \rceil$ indicates the smallest integer number bigger than x, and each user interferes with the desired user with probability 1/2. Therefore, the probability that l users effectively interfere with the desired user can be expressed as

$$P_{\text{Sync}}(l) = \binom{\lceil \frac{U}{K} \rceil - 1}{l}\left(\frac{1}{2}\right)^{\lceil \frac{U}{K} \rceil - 1} \tag{13}$$

and the BER of the system is as follows:

$$\text{BER} = \sum_{l=0}^{\lceil \frac{U}{K} \rceil - 1} P_{\text{Sync}}(l)\text{BER}(l). \tag{14}$$

Note that when the duration of integration time (T) is more than the spreading time (N_0T_c), the integration time can be divided into two parts: one with interfering user's pulse and the other without this interfering pulse. The power spectral density of the first part is equal to the sum of the power spectral densities due to amplification noise and interfering users' pulse, while the power spectral density of the second part is less than the first part due to less number of interfering users. This leads to the power spectral density being less than the value predicted in (3); therefore, the BER derived in this paper can be considered to be an upper bound for such cases. This is the case when the complete duration of incorrectly decoded pulse does not exist in the integration time period.

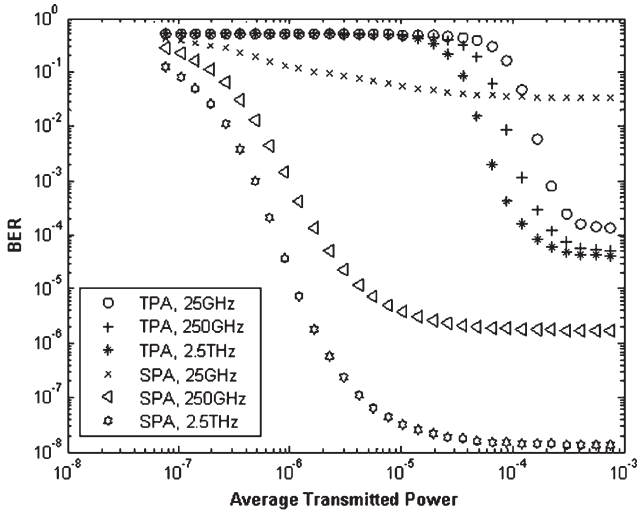

Fig. 3. BER versus average transmitted power for asynchronous transmitters using TPA and SPA receivers with different photodetector speed.

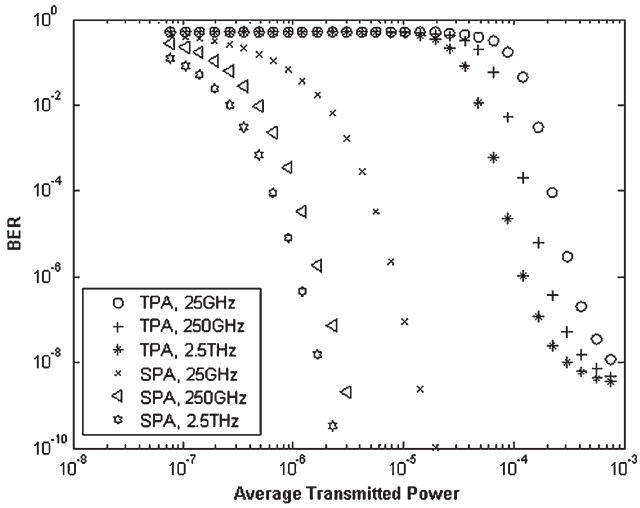

Fig. 4. BER versus average transmitted power for slot-level synchronous transmitters using TPA and SPA receivers with different photodetector speed.

C. Numerical Discussion

The BER for different cases is sketched in Figs. 3–12 using the parameters specified in Table I (unless the values of parameters that are specified in the text). As discussed in Appendix B in this paper, the simplified approach, where most of the energy of the decoded pulse is assumed to be within a chip time, introduced in [19], is used for the performance analysis of TPA receivers.

The BER of a typical spectral-phase-encoded optical CDMA system with SPA and TPA receivers and asynchronous transmitters with various photodetector speeds is sketched in Fig. 3. As shown in this figure, the performance of the SPA receiver

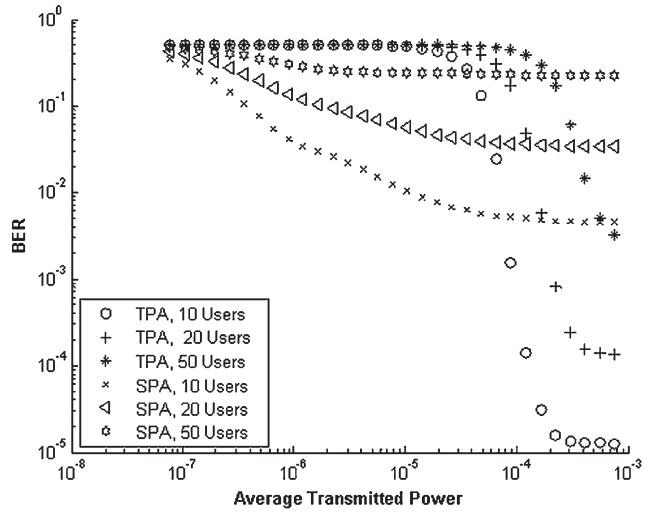

Fig. 5. BER versus average transmitted power for asynchronous transmitters using TPA and SPA receivers with different number of users with a photodetector speed of 25 GHz.

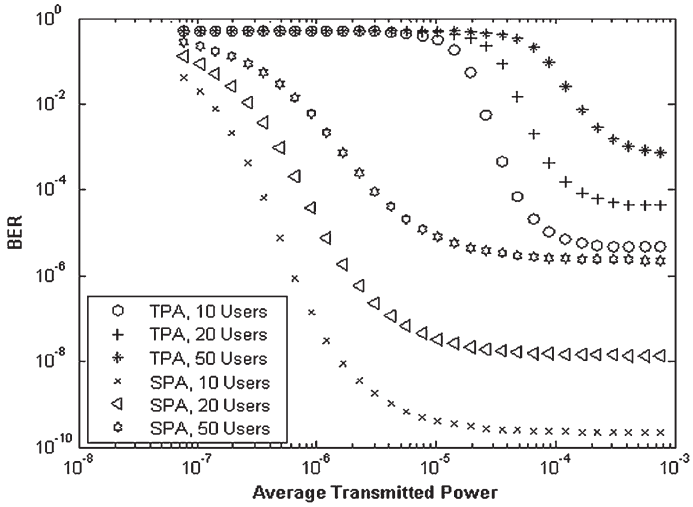

Fig. 6. BER versus average transmitted power for asynchronous transmitters using TPA and SPA receivers with different number of users with a photodetector speed of 2.5 THz.

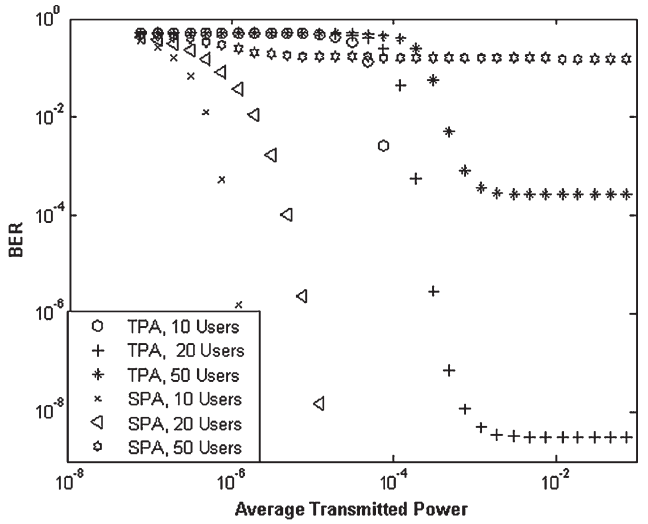

Fig. 7. BER versus average transmitted power for slot-level synchronous transmitters using TPA and SPA receivers with different number of users with a photodetector speed of 25 GHz.

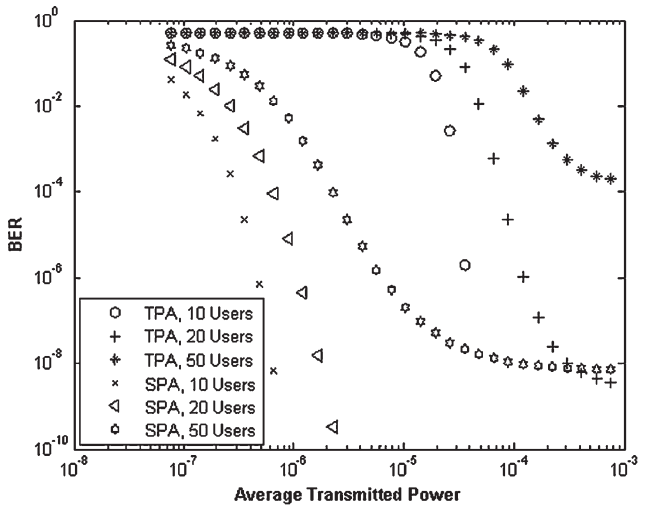

Fig. 8. BER versus average transmitted power for slot-level synchronous transmitters using TPA and SPA receivers with different number of users with a photodetector speed of 2.5 THz.

is superior to the TPA receiver (with respect to BER) when an ideal optical gating device with integration time that can be as low as the chip time (ideal case) is used. This, in turn, requires the use of a sophisticated time gating, which increases the complexity and the cost of femto- or picosecond-based optical CDMA receivers. However, as the integration time increases, i.e., using lower speed photodetectors, the performance of TPA receivers surpasses that of the SPA. As it is shown in Fig. 3, the performance of the TPA receiver is much more superior to that of the SPA receiver when a typical photodetector with a speed of 25 GHz is used.

The BER for the same system, as in Fig. 3, with slot-level synchronous transmitters is sketched in Fig. 4. As observed in this figure, SPA receivers obtain better performance as compared to TPA receivers. This is due to the fact that the spreading is equal to 250 and that the number of effective interferers in this configuration is equal to 1. Therefore, by even using a 25-GHz receiver (integrating over 100 chip times), one can easily distinguish between the correctly decoded and incorrectly decoded pulses using an SPA detector.

Figs. 5 and 6 show the BER of the system with different number of users for asynchronous receiver with 25-GHz and 2.5-THz speed photodetector. As one expects, the BER of the system improves as the number of users decreases for both cases. This is the case in Figs. 7 and 8, where slot-level synchronization between transmitters has been considered. From these figures, it is observed that as the number of users increases, e.g., 50 users for 25-GHz receiver, using the TPA receiver performs better than the SPA receiver, as in asynchronous receiver. This is due to the fact that the large number of simultaneous interferers leads to a more average power in low-speed detectors and, hence, increases the BER for SPA receivers.

Figs. 9 and 10 show the BER of the system with different code lengths for the system using asynchronous transmitter with low- and high-speed photodetectors. As expected, the performance of the system improves as the code length

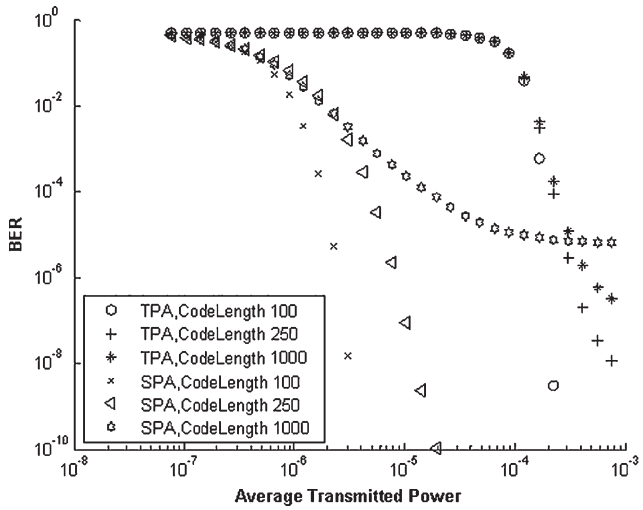

Fig. 9. BER versus average transmitted power for asynchronous transmitters using TPA and SPA receivers with different code lengths with a photodetector speed of 25 GHz.

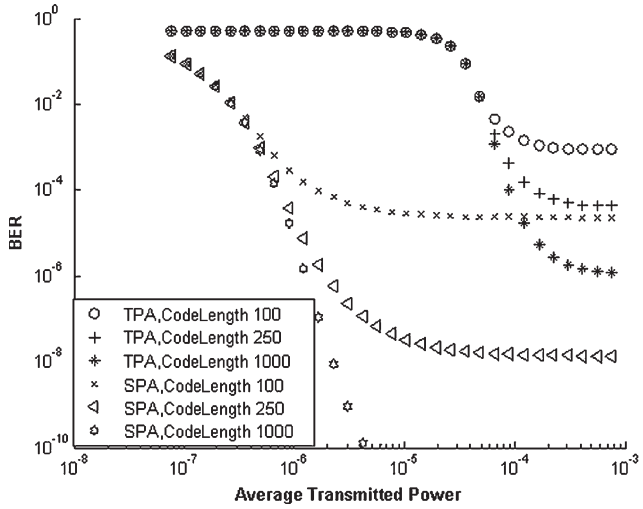

Fig. 10. BER versus average transmitted power for asynchronous transmitters using TPA and SPA receivers with different code lengths with a photodetector speed of 2.5 THz.

increases. As before, the performance of the TPA receiver is better when using low-speed photodetectors, while the SPA receiver performs better when a high-speed photodetector is used.

The BER of the same systems, as shown in Figs. 9 and 10 but with slot-level synchronization, is sketched in Figs. 11 and 12. It is shown in these figures that by increasing the code length, the performance of the system does not improve. This is due to the fact that when there are slot-level synchronous transmitters, the number of interfering users is equal to U/K. In our numerical evaluation, the bit rate and chip time are fixed; therefore, the product $KN_0 = T_b/T_c$ is held constant. Thus, increasing N_0, the value for K decreases. This leads to more interferers in the slot-level synchronous transmission when higher value of N_0 is used; therefore, the BER becomes worse. It should be mentioned that by decreasing the chip time, we can reach higher bit rates or use higher code lengths to increase the number of users.

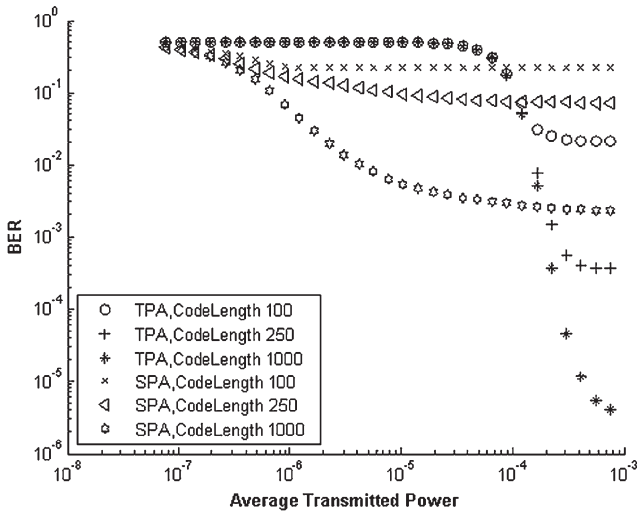

Fig. 11. BER versus average transmitted power for slot-level synchronous transmitters using TPA and SPA receivers with different code lengths with a photodetector speed of 25 GHz.

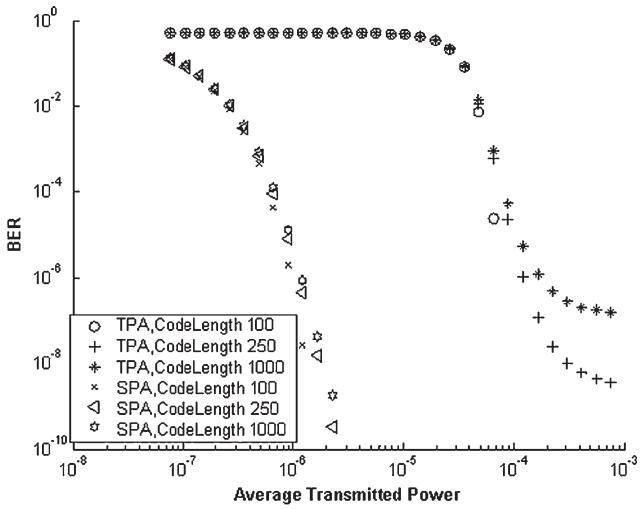

Fig. 12. BER versus average transmitted power for slot-level synchronous transmitters using TPA and SPA receivers with different code lengths with a photodetector speed of 2.5 THz.

V. Conclusion

In this paper, we obtained the performance of the spectral-phase-encoded optical CDMA systems using SPA and TPA receiver structures with asynchronous and slot-level synchronous transmitters. It is shown that using the TPA receiver is beneficial when typical photodetectors with ordinary speeds are used in the system. Although using the slot-level synchronization among transmitters is more complex, it leads to a better performance of the system due to the decrease in total interference in the system.

Appendix A

In this Appendix, we obtain the mean and the variance of the received signal using a method described in [17]. By using (1) and assuming that both MAI and amplification noise have

TABLE I
TYPICAL VALUES USED IN THIS PAPER

n_{sp}	*Spontaneous Emission Factor*	1.1
T_r	*Receiver Temperature*	300° *K*
R_L	*Load Resistance*	1000 Ω
T_c	*width of ultrashort pulse*	400*fsec*
η	*Quantum Efficiency*	0.9
k_3	*Detection Efficiency in TPA receiver*	5.0 *e* -11 for T_c
N_0	*Code Length*	250
U	*Number of Users*	20
R	*Bit Rate*	1 Gbps
G_{amp}	*Gain of Amplifier*	1000 (30 dB)
L_1	*Total path loss before amplification*	8 dB
L_2	*Total path loss after amplification*	5 dB

Gaussian distribution and are mutually statistically independent, the received signal at the receiver can be described as

$$\begin{aligned} r(t) &= \sqrt{G}E_{ii}(t) + \sqrt{G}\sum_{j\neq i}^{U} E_{ij}(t) + Q(t) \\ &= \sqrt{G}E_{ii}(t) + B(t) \end{aligned} \tag{A.1}$$

where $B(t)$ is a Gaussian random variable with power spectral density equal to the sum of the power spectral densities of MAI $\sqrt{G}\sum_{j\neq i}^{U} E_{ij}(t)$ and amplification noise $Q(t)$, which can be written as

$$N_S = N_T + l\frac{mG}{N_0} \tag{A.2}$$

where l is the number of interfering users. We assume that the received signal field $r(t)$ can be expressed as a slowly varying signal $F(t)$ multiplied by a carrier with frequency of light [19], i.e.,

$$r(t) = F(t)\cos(2\pi ft + \varphi) \tag{A.3}$$

where φ is the phase of the received signal. Accordingly, the slowly varying terms of the correctly decoded signal $\sqrt{G}E_{ii}(t)$ and Gaussian random variable at the receiver $B(t) = \sqrt{G}\sum_{j\neq i}^{U} E_{ij}(t) + Q(t)$ can be expressed as

$$\sqrt{G}E_{ii}(t) = C(t)\cos(2\pi ft + \varphi) \tag{A.4}$$

$$B(t) = D(t)\cos(2\pi ft + \varphi) \tag{A.5}$$

where $C(t)$ and $D(t)$ are the base-band representations of $\sqrt{G}E_{ii}(t)$ and $B(t)$, respectively. Therefore, the received number of photoelectrons in the detector $Y_{i,\mathrm{SPA}}$ can be expressed as

$$Y_{i,\mathrm{SPA}} = \frac{\eta}{2}\int_0^T |C(t) + D(t)|^2\, dt \tag{A.6}$$

where T is the integration time of the receiver. By using M modes for the received signal, the base-band representations of the correctly decoded signal and the Gaussian random variable due to amplification and MAI can be described by their Fourier series expansions as [17]

$$C(t) = \sum_{n=1}^{M} a_n e^{jn\Omega t} \tag{A.7}$$

$$D(t) = \sum_{n=1}^{M} x_n e^{jn\Omega t} \tag{A.8}$$

where $\Omega = 2\pi/T$, a_n is the Fourier series coefficient for $C(t)$, and x_n is the complex Fourier series coefficient for $D(t)$. By substituting (A.7) and (A.8) in (A.6), the received signal can be expressed as

$$Y_{i,\mathrm{SPA}} = \frac{\eta T}{2}\sum_{n=1}^{M}\left((a_n + x_{\mathrm{cn}})^2 + x_{\mathrm{sn}}^2\right). \tag{A.9}$$

By using (A.9), the mean and the variance of the received photoelectrons at the photodetector can be expressed as (4) and (5) [17].

APPENDIX B

In this Appendix, we derive the mean and the variance of the received signal by the TPA receiver. Assuming the same conditions as specified for the SPA receiver, the received signal at the input of a TPA receiver can be expressed as (A.1). Assuming an ideal TPA receiver, i.e., $\alpha = 0$, the received number of photoelectrons in TPA can be expressed as [19]

$$Y_{i,\mathrm{TPA}} = k_2\int_0^T |F(t)|^4\, dt \tag{B.1}$$

where k_2 is a constant equal to $3Vhf\gamma/16S^2$ [19]. V is the volume of the detector, and S is the area of the TPA photodetector. By substituting (A.7) and (A.8) in the above equation, the received signal can be expressed as [19]

$$\begin{aligned} &Y_{i,\mathrm{TPA}} \\ &= k_2 T \sum_{\substack{m,n,p,q=1 \\ m+n-p-q=0}}^{M} ((a_m + q_m)(a_n + q_n)(a_p + q_p)^*(a_q + q_q)^*). \end{aligned} \tag{B.2}$$

Obtaining the mean and the variance of the above value is intractable for arbitrary pulse shapes. In a simplified approach introduced in [19], the integration time is divided into M intervals where only one interval contains signal plus noise and the rest, i.e., the $M-1$ intervals, contain noise only. Assuming that the signal exists on the first interval, (B.2) can be simplified to

$$\begin{aligned} Y_{\mathrm{TPA}} = k_2 T_c \Bigg[&\left((a_1 + x_{c1})^4 + x_{s1}^4 + 2(a_1 + x_{c1})^2 x_{s1}^2\right) \\ &+ \sum_{n=2}^{M}\left(x_{\mathrm{cn}}^4 + x_{\mathrm{sn}}^4 + 2x_{\mathrm{cn}}^2 x_{\mathrm{sn}}^2\right)\Bigg]. \end{aligned} \tag{B.3}$$

Therefore, the mean and the variance of the received signal in (B.3) can be obtained as described in [19], which lead us to (7) and (8).

REFERENCES

[1] H. Shinohara, "Broadband access in Japan: Rapidly growing FTTH market," *IEEE Commun. Mag.*, vol. 43, no. 9, pp. 72–78, Sep. 2005.

[2] S. Cherry, "A broadband Utopia," *IEEE Spectr.*, vol. 43, no. 5, pp. 48–54, May 2006.

[3] B. T. Coonen, "Fiber to the home / fiber to the premises: What, where, and when?" *Proc. IEEE*, vol. 94, no. 5, pp. 911–934, May 2006.

[4] J. Ratnam, "Optical CDMA in broadband communication: Scope and applications," *J. Opt. Commun.*, vol. 23, no. 1, pp. 11–21, Jan. 2002.

[5] J. A. Salehi, A. M. Weiner, and J. P. Heritage, "Coherent ultrashort light pulse code-division multiple access communication systems," *J. Lightw. Technol.*, vol. 8, no. 3, pp. 478–491, Mar. 1990.

[6] M. Rochette and L. A. Rusch, "Spectral efficiency of OCDMA systems with coherent pulsed sources," *J. Lightw. Technol.*, vol. 23, no. 3, pp. 1033–1038, Mar. 2005.

[7] T. H. Shake, "Confidentiality performance of spectral-phase-encoded optical CDMA," *J. Lightw. Technol.*, vol. 23, no. 4, pp. 1652–1663, Apr. 2005.

[8] Z. Jiang, D. S. Seo, S. D. Yang, D. E. Leaird, R. V. Roussev, C. Langrock, M. M. Fejer, and A. M. Weiner, "Four-user, 2.5 Gb/s, spectrally coded OCDMA system demonstration using low-power nonlinear processing," *J. Lightw. Technol.*, vol. 23, no. 1, pp. 143–158, Jan. 2005.

[9] Z. Zheng, H. Sardesai, C. C. Chang, S. Shen, A. M. Weiner, J. H. Marsh, and M. M. Kharkhanehchi, "Nonlinear detection of spectrally coded ultrashort pulse by two-photon absorption GaAs waveguide photodetectors," in *Proc. CLEO*, May 18–23, 1997, vol. 11, pp. 165–166.

[10] Z. Zheng, A. M. Weiner, J. H. Marsh, and M. M. Karkhanehchi, "Ultrafast optical thresholding based on two-photon absorption GaAs waveguide photodetectors," *IEEE Photon. Technol. Lett.*, vol. 9, no. 4, pp. 493–495, Apr. 1997.

[11] K. Jamshidi and J. A. Salehi, "Statistical analysis of coherent ultrashort light pulse CDMA with multiple optical amplifiers using additive noise model," *J. Lightw. Technol.*, vol. 23, no. 5, pp. 1842–1851, May 2005.

[12] H. P. Sardesai, C. C. Chang, and A. M. Weiner, "A femtosecond code-division multiple-access communication system test bed," *J. Lightw. Technol.*, vol. 16, no. 11, pp. 1953–1964, Nov. 1998.

[13] S. Etemad, P. Toliver, R. Menendez, J. Young, T. Banwell, S. Galli, J. Jackel, P. Delfyett, C. Price, and T. Turpin, "Spectrally efficient optical CDMA using coherent phase-frequency coding," *IEEE Photon. Technol. Lett.*, vol. 17, no. 4, pp. 929–931, Apr. 2005.

[14] R. P. Scott, W. Cong, K. Li, V. J. Hernandez, B. H. Kolner, J. P. Heritage, and S. J. B. Yoo, "Demonstration of an error-free 4/spl times/10Gb/s multiuser SPECTS O-CDMA network testbed," *IEEE Photon. Technol. Lett.*, vol. 16, no. 9, pp. 2186–2188, Sep. 2004.

[15] V. J. Hernandez, D. Yixue, W. Cong, R. P. Scott, K. Li, J. P. Heritage, D. Zhi, B. H. Kolner, and S. J. B. Yoo, "Spectral phase-encoded time-spreading (SPECTS) optical code-division multiple access for terabit optical access networks," *J. Lightw. Technol.*, vol. 22, no. 11, pp. 2671–2679, Nov. 2004.

[16] R. P. Scott, W. Cong, V. J. Hernandez, K. Li, B. H. Kolner, J. P. Heritage, and S. J. B. Yoo, "An eight-user time-slotted SPECTS O-CDMA testbed: Demonstration and simulations," *J. Lightw. Technol.*, vol. 23, no. 10, pp. 3232–3240, Oct. 2005.

[17] G. Einarsson, *Principles of Lightwave Communications*. Hoboken, NJ: Wiley, 1996.

[18] P. J. Maguire, L. P. Barry, T. Krug, M. Lynch, A. L. Bradley, J. F. Donegan, and H. Folliot, "All-optical sampling utilizing two-photon absorption in semiconductor microcavity," *Electron. Lett.*, vol. 41, no. 8, pp. 489–490, Apr. 2005.

[19] K. Jamshidi and J. A. Salehi, "Statistical characterization and bit-error rate analysis of lightwave systems with optical amplification using two-photon absorption receiver structures," *J. Lightw. Technol.*, vol. 24, no. 3, pp. 1302–1316, Mar. 2006.

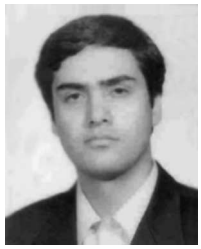

Kambiz Jamshidi (S'06–M'07) was born in Tehran, Iran, on April 3, 1977. He received the B.S., M.S., and Ph.D. degrees in electrical engineering from Sharif University of Technology (SUT), Tehran, in 1999, 2001, and 2006, respectively.

He is currently with the Optical Networks Research Lab (ONRLab) as a Faculty member of the Advanced Communications Research Institute (ACRI), SUT. From August 2000 to August 2001, he was a member of research staff with the Advanced CDMA Research Laboratory, Iran Telecommunication Research Center (ITRC), Tehran. From March 2002 to March 2004, he was a member of research staff with Mobile Communications Division, ITRC. From October 2005 to March 2006, he was a Research Assistant with the HFT Department, Technical University Berlin, Berlin, Germany. His research interests include optical communication systems, specifically, optical CDMA and WDM systems, optical transmission systems, applications of optical amplifiers in optical networks, and mathematical modeling of optical devices used in optical communication systems.

Jawad A. Salehi (M'02–SM'07) was born in Kazemain, Iraq, on December 22, 1956. He received the B.S. degree in electrical engineering from the University of California, Irvine, in 1979 and the M.S. and Ph.D. degrees in electrical engineering from University of Southern California (USC), Los Angeles, in 1980 and 1984, respectively.

From 1981 to 1984, he was a full-time Research Assistant with Communication Science Institute at USC, where he was engaged in research in the area of spread spectrum systems. From 1984 to 1993, he was a member of technical staff of the Applied Research Area, Bell Communications Research (Bellcore), Morristown, NJ. From February to May 1990, he was with the Laboratory of Information and Decision Systems, Massachusetts Institute of Technology (MIT), Cambridge, as a Visiting Research Scientist, where he was conducting research on optical multiple-access networks. He was an Associate Professor from 1997 to 2003 and is currently a Full Professor with the Electrical Engineering (EE) Department, Sharif University of Technology (SUT), Tehran, Iran. From 1999 to 2001, he was the Head of Mobile Communications Systems Group and Codirector of Advanced and Wideband Code Division Multiple Access (CDMA) Laboratory, Iran Telecom Research Center (ITRC), Tehran, where he was conducting a research in the area of advance CDMA techniques for optical and radio communications systems. From 2003 to 2006, he was the Director of the National Center of Excellence in Communications Science, EE Department, SUT. In 2003, he founded and directed the Optical Networks Research Laboratory (ONRL), Electrical Engineering Department, SUT, for advanced theoretical and experimental research in futuristic all-optical networks. He is also a Cofounder of Advanced Communications Research Institute (ACRI), SUT, for advancing the graduate school research program in communications science. His current research interests include optical multiaccess networks, in particular, optical orthogonal codes (OOC); fiber-optic CDMA; femtosecond or ultrashort light pulse CDMA; spread time CDMA; holographic CDMA; wireless indoor optical CDMA; all-optical synchronization; and applications of erbium-doped fiber amplifiers (EDFAs) in optical systems. He is the holder of 12 U.S. patents on optical CDMA.

Dr. Salehi was a recipient of the Bellcore's Award of Excellence, the Outstanding Research Award of the EE Department of SUT in 2002, 2003, and 2006, the Outstanding Research Award of SUT 2003, the Nationwide Outstanding Research Award from the Ministry of Higher Education 2003, and the Nation's Highly Cited Researcher Award 2004. Recently, he was introduced as among the 250 pre-eminent and most influential researchers worldwide by the Institute for Scientific Information (ISI), highly cited in the computer-science category. He was the corecipient of IEEE's Best Paper Award ("spread-time/time-hopping ultrawideband (UWB) CDMA communications systems") from the International Symposium on Communications and Information Technology, October 2004, Japan. He was also the recipient of the first rank in fundamental research of the Khwarizmi International Prize and the recipient of World Intellectual Propriety Organization (WIPO) award for outstanding inventor for 2007. He was a member of the organizing committee for the first and the second IEEE Conference on Neural Information. Since May 2001, he has been serving as the Associate Editor for optical CDMA for the IEEE TRANSACTIONS ON COMMUNICATIONS. In September 2005, he was elected as the interim Chair of the IEEE Iran section.